BRIEF REPORT

Zika Virus Associated with Microcephaly

Jernej Mlakar, M.D., Misa Korva, Ph.D., Nataša Tul, M.D., Ph.D., Mara Popović, M.D., Ph.D., Mateja Poljšak-Prijatelj, Ph.D., Jerica Mraz, M.Sc., Marko Kolenc, M.Sc., Katarina Resman Rus, M.Sc., Tina Vesnaver Vipotnik, M.D., Vesna Fabjan Vodušek, M.D., Alenka Vizjak, Ph.D., Jože Pižem, M.D., Ph.D., Miroslav Petrovec, M.D., Ph.D., and Tatjana Avšič Županc, Ph.D.

SUMMARY

A widespread epidemic of Zika virus (ZIKV) infection was reported in 2015 in South and Central America and the Caribbean. A major concern associated with this infection is the apparent increased incidence of microcephaly in fetuses born to mothers infected with ZIKV. In this report, we describe the case of an expectant mother who had a febrile illness with rash at the end of the first trimester of pregnancy while she was living in Brazil. Ultrasonography performed at 29 weeks of gestation revealed microcephaly with calcifications in the fetal brain and placenta. After the mother requested termination of the pregnancy, a fetal autopsy was performed. Micrencephaly (an abnormally small brain) was observed, with almost complete agyria, hydrocephalus, and multifocal dystrophic calcifications in the cortex and subcortical white matter, with associated cortical displacement and mild focal inflammation. ZIKV was found in the fetal brain tissue on reverse-transcriptase–polymerase-chain-reaction (RT-PCR) assay, with consistent findings on electron microscopy. The complete genome of ZIKV was recovered from the fetal brain.

ZIKV, AN EMERGING MOSQUITO-BORNE FLAVIVIRUS, WAS INITIALLY ISOlated from a rhesus monkey in the Zika forest in Uganda in 1947.[1] It is transmitted by various species of aedes mosquitoes. After the first human ZIKV infection, sporadic cases were reported in Southeast Asia and sub-Saharan Africa.[2] ZIKV was responsible for the outbreak in Yap Island of Micronesia in 2007 and for major epidemics in French Polynesia, New Caledonia, the Cook Islands, and Easter Island in 2013 and 2014.[3,4] In 2015, there was a dramatic increase in reports of ZIKV infection in the Americas. Brazil is the most affected country, with preliminary estimates of 440,000 to 1.3 million cases of autochthonous ZIKV infection reported through December 2015.[5]

The classic clinical picture of ZIKV infection resembles that of dengue fever and chikungunya and is manifested by fever, headache, arthralgia, myalgia, and maculopapular rash, a complex of symptoms that hampers differential diagnosis. Although the disease is self-limiting, cases of neurologic manifestations and the Guillain–Barré syndrome were described in French Polynesia and in Brazil during ZIKV epidemics.[5,6] Recent reports from the Ministry of Health of Brazil suggest that cases of microcephaly have increased by a factor of approximately 20 among newborns in the northeast region of the country, which indicates a possible association between ZIKV infection in pregnancy and fetal malformations.[5]

We present a case of vertical transmission of ZIKV in a woman who was prob-

From the Institute of Pathology, Faculty of Medicine (J. Mlakar, M. Popović, J. Mraz, A.V., J.P.), and the Institute of Microbiology and Immunology, Faculty of Medicine (M. Korva, M.P.-P., M. Kolenc, K.R.R., M. Petrovec, T.A.Z.), University of Ljubljana, and the Department of Perinatology, Division of Gynecology and Obstetrics (N.T., V.F.V.), and the Institute of Radiology (T.V.V.), University Medical Center Ljubljana — all in Ljubljana, Slovenia. Address reprint requests to Dr. Avšič Županc at the Institute of Microbiology and Immunology, Faculty of Medicine, University of Ljubljana, Zaloška 4, Ljubljana 1000, Slovenia, or at tatjana.avsic@mf.uni-lj.si.

This article was published on February 10, 2016, at NEJM.org.

DOI: 10.1056/NEJMoa1600651

Copyright © 2016 Massachusetts Medical Society.

The New England Journal of Medicine
Downloaded from nejm.org on February 19, 2016. For personal use only. No other uses without permission.
Copyright © 2016 Massachusetts Medical Society. All rights reserved.

ably infected with ZIKV in northeastern Brazil at the end of the first trimester of pregnancy. Our discussion includes details of fetal imaging and pathological and virologic analyses.

CASE REPORT

In mid-October 2015, a 25-year-old previously healthy European woman came to the Department of Perinatology at the University Medical Center in Ljubljana, Slovenia, because of assumed fetal anomalies. Since December 2013, she had lived and worked as a volunteer in Natal, the capital of Rio Grande do Norte state. She had become pregnant at the end of February 2015. During the 13th week of gestation, she had become ill with high fever, which was followed by severe musculoskeletal and retroocular pain and an itching, generalized maculopapular rash. Since there was a ZIKV epidemic in the community, infection with the virus was suspected, but no virologic diagnostic testing was performed. Ultrasonography that was performed at 14 and 20 weeks of gestation showed normal fetal growth and anatomy.

The patient returned to Europe at 28 weeks of gestation. Ultrasonographic examination that was performed at 29 weeks of gestation showed the first signs of fetal anomalies, and she was referred to the Department of Perinatology. At that time, she also noticed reduced fetal movements. Ultrasonography that was performed at 32 weeks of gestation confirmed intrauterine growth retardation (estimated third percentile of fetal weight) with normal amniotic fluid, a placenta measuring 3.5 cm in thickness (normal size) with numerous calcifications, a head circumference below the second percentile for gestation (microcephaly), moderate ventriculomegaly, and a transcerebellar diameter below the second percentile. Brain structures were blurred, and there were numerous calcifications in various parts of the brain (Fig. 1A and 1B). There were no other obvious fetal structural abnormalities. Fetal, umbilical, and uterine blood flows were normal on Doppler ultrasonography.

The clinical presentation raised suspicion of fetal viral infection. Because of severe brain disease and microcephaly, the fetus was given a poor prognosis for neonatal health. The mother requested that the pregnancy be terminated, and the procedure was subsequently approved by national and hospital ethics committees. Medical termination of the pregnancy was performed at 32 weeks of gestation. At the delivery, the only morphologic anomaly was the prominent microcephaly. Genetic consultation that included a detailed maternal family history revealed no suspicion of genetic syndromes or diseases. An autopsy was performed, as is mandatory in all cases of termination of pregnancy. The mother provided written informed consent for the publication of this case report.

METHODS

AUTOPSY AND CENTRAL NERVOUS SYSTEM (CNS) EXAMINATION

An autopsy of the fetus and placenta was performed 3 days after termination of the pregnancy, with an extensive sampling of all organs, placenta, and umbilical cord. Samples were fixed in 10% buffered formalin and embedded in paraffin. Fresh tissue samples were collected for microbiologic investigations. Brain and spinal cord were fixed in 27% buffered formalin for 3 weeks, after which a neuropathological examination was performed with extensive sampling of the brain and spinal cord. Sections of all tissue samples were stained with hematoxylin and eosin. Immunostaining for glial fibrillary acid protein, neurofilament, human leukocyte antigen DR (HLA-DR), CD3 (to highlight T cells), and CD20 (to highlight B cells) was performed on representative CNS samples.

ELECTRON MICROSCOPY

Tissue was collected from formalin-fixed brain and underwent fixation in 1% osmium tetroxide and dehydration in increasing concentrations of ethanol. The sample was then embedded in Epon. Semithin sections (1.4 μm) were made, stained with Azur II, and analyzed by means of light microscopy. Ultrathin sections (60 nm) were stained with uranyl acetate and lead citrate. In addition, a small piece of brain (5 mm^3) was homogenized in buffer. The suspension was then cleared by low-speed centrifugation, and the obtained supernatant was ultracentrifuged directly onto an electron microscopic grid with the use of an Airfuge (Beckman Coulter). Negative staining was performed with 1% phosphotungstic acid. Imaging of the ultrathin sections and brain homogenate was performed with the use of a 120-kV JEM-1400Plus transmission electron microscope (JEOL).

The New England Journal of Medicine
Downloaded from nejm.org on February 19, 2016. For personal use only. No other uses without permission.
Copyright © 2016 Massachusetts Medical Society. All rights reserved.

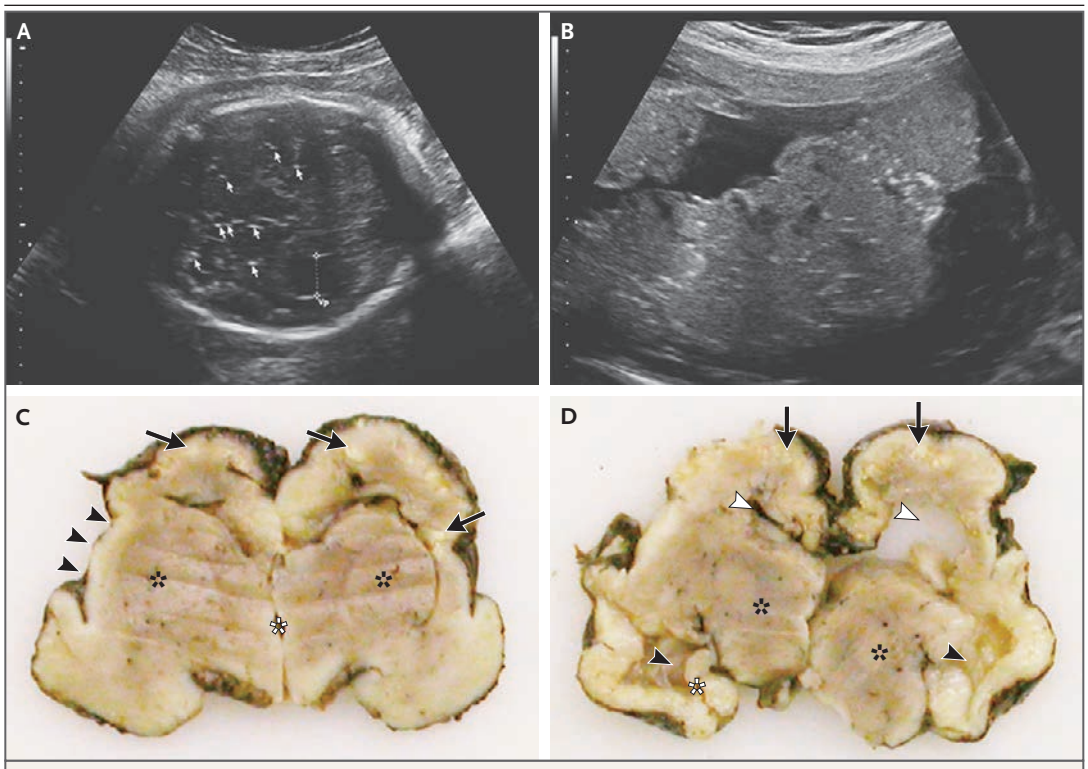

Figure 1. Prenatal Ultrasonographic Images and Photographs of Coronal Slices of Brain.

Panel A shows numerous calcifications in various parts of the brain (some marked with arrows) and the dilated occipital horn of the lateral ventricle (Vp, marked with a measurement bar) as seen on transverse ultrasonography. Panel B shows numerous calcifications in the placenta. Panel C shows multifocal cortical and subcortical white calcifications (arrows) and almost complete loss of gyration of the cortex. The basal ganglia are developed but poorly delineated (black asterisks), and the sylvian fissures are widely open on both sides (arrowheads on the left). The third ventricle is not dilated (white asterisk). Panel D shows dilated body of the lateral ventricles (white arrowheads); the left is collapsed. Temporal horns of the lateral ventricles (black arrowheads) are also dilated. The thalami (black asterisks) and the left hippocampus (white asterisk) are well developed, whereas the contralateral structure is not recognizable owing to autolysis.

INDIRECT IMMUNOFLUORESCENCE

Paraffin-embedded sections of the fetal brain tissue and brain tissue of an autopsied man as a negative control were incubated with serum obtained from the mother of the fetus (dilution, 1:10), followed by antihuman IgG antibodies labeled with fluorescein isothiocyanate (FITC) (dilution, 1:50). In addition, fetal brain tissue was incubated with a serum obtained from a healthy blood donor, as well as with FITC-labeled antihuman IgG antibodies only.

MICROBIOLOGIC INVESTIGATION

RNA was extracted from 10 mg of the placenta, lungs, heart, skin, spleen, thymus, liver, kidneys, and cerebral cortex with the use of a TRIzol Plus RNA purification kit (Thermo Fisher Scientific). Real-time RT-PCR for the detection of ZIKV RNA (NS5) and one-step RT-PCR for the detection of the envelope-protein coding region (360 bp) were performed as described previously.[7,8] In addition, next-generation sequencing was performed in samples of fetal brain tissue with the use of Ion Torrent (Thermo Fisher Scientific) and Geneious software, version 9.0.6. Reads from both runs were combined and mapped to the reference sequence (ZIKV MR766; LC002520) with the use of default measures. For phylogenetic analysis, complete-genome ZIKV sequences were used, and multiple sequence alignments (ClustalW) were performed. A neighbor-joining phylogenetic tree (GTR+G+I model) was constructed, with the use of the MEGA6 software system,[9] to show the phylogenetic relationships. The nucleotide sequence of ZIKV that was obtained in this study has been deposited in GenBank

The New England Journal of Medicine
Downloaded from nejm.org on February 19, 2016. For personal use only. No other uses without permission.
Copyright © 2016 Massachusetts Medical Society. All rights reserved.

under accession number KU527068. A detailed description of the molecular methods is provided in the Supplementary Appendix, available with the full text of this article at NEJM.org. The results of comprehensive serologic analyses of maternal serum and a description of the molecular differential diagnostic procedures used with fetal tissue samples are provided in Tables S1 and S2 in the Supplementary Appendix. All the authors vouch for the completeness and accuracy of the data and analyses presented.

RESULTS

AUTOPSY AND NEUROPATHOLOGICAL FINDINGS

The fetal body weight was 1470 g (5th percentile), the length 42 cm (10th percentile), and the head circumference 26 cm (1st percentile). The only external anomaly that was noted was microcephaly. The placenta weighed 200 g, resulting in a placental–fetal weight ratio of 0.136 (<3rd percentile). Macroscopic examination of the CNS revealed micrencephaly with a whole-brain weight of 84 g (4 SD below average), widely open sylvian fissures, and a small cerebellum and brain stem. Almost complete agyria and internal hydrocephalus of the lateral ventricles were observed. There were numerous variable-sized calcifications in the cortex and subcortical white matter in the frontal, parietal, and occipital lobes. The subcortical nuclei were quite well developed (Fig. 1C and 1D). In spite of some autolysis, microscopic examination revealed appropriate cytoarchitecture of the fetal brain. The most prominent histopathological features were multifocal collections of filamentous, granular, and neuron-shaped calcifications in the cortex and subcortical white matter with focal involvement of the whole cortical ribbon, occasionally associated with cortical displacement (Fig. 2A and 2B). Diffuse astrogliosis was present with focal astrocytic outburst into the subarachnoid space, mostly on the convexity of the cerebral hemispheres (Fig. 2C). Activated microglial cells and some macrophages expressing HLA-DR were present throughout most of the cerebral gray and white matter (Fig. 2D). Scattered mild perivascular infiltrates composed of T cells and some B cells were present in the subcortical white matter (Fig. S1 in the Supplementary Appendix). The cerebellum, brain stem, and spinal cord showed neither inflammation nor dystrophic calcifications. The brain stem and spinal cord showed Wallerian degeneration of the long descending tracts, especially the lateral corticospinal tract, whereas ascending dorsal columns were well preserved (Fig. 2E). Indirect immunofluorescence revealed granular intracytoplasmic reaction in destroyed neuronal structures, which pointed to a possible location of the virus in neurons (Fig. 2F, and Fig. S1 in the Supplementary Appendix). Histologic examination of the placenta confirmed focal calcifications in villi and decidua, but no inflammation was found. There were no relevant pathological changes in other fetal organs or in the umbilical cord or fetal membranes. Fetal karyotyping with the use of microarray technology showed a normal 46XY (male) profile.

ELECTRON MICROSCOPY

Although analysis of the ultrathin sections of the brain showed poorly preserved brain tissue with ruptured and lysed cells, clusters of dense virus-like particles of approximately 50 nm in size were found in damaged cytoplasmic vesicles. Groups of enveloped structures with a bright interior were also detected. At the periphery of such groups, the remains of membranes could be seen. Negative staining of homogenized brain revealed spherical virus particles measuring 42 to 54 nm with morphologic characteristics consistent with viruses of the Flaviviridae family (Fig. 3).

MICROBIOLOGIC INVESTIGATION

Positive results for ZIKV were obtained on RT-PCR assay only in the fetal brain sample, where 6.5×10^7 viral RNA copies per milligram of tissue were detected. In addition, all autopsy samples were tested on PCR assay and were found to be negative for other flaviviruses (dengue virus, yellow fever virus, West Nile virus, and tick-borne encephalitis virus), along with chikungunya virus, lymphocytic choriomeningitis, cytomegalovirus, rubella virus, varicella–zoster virus, herpes simplex virus, parvovirus B19, enteroviruses, and *Toxoplasma gondii* (Table S2 in the Supplementary Appendix).

A complete ZIKV genome sequence (10,808 nucelotides) was recovered from brain tissue. Phylogenetic analysis showed the highest identity (99.7%) with the ZIKV strain isolated from a patient from French Polynesia in 2013 (KJ776791)

The New England Journal of Medicine
Downloaded from nejm.org on February 19, 2016. For personal use only. No other uses without permission.
Copyright © 2016 Massachusetts Medical Society. All rights reserved.

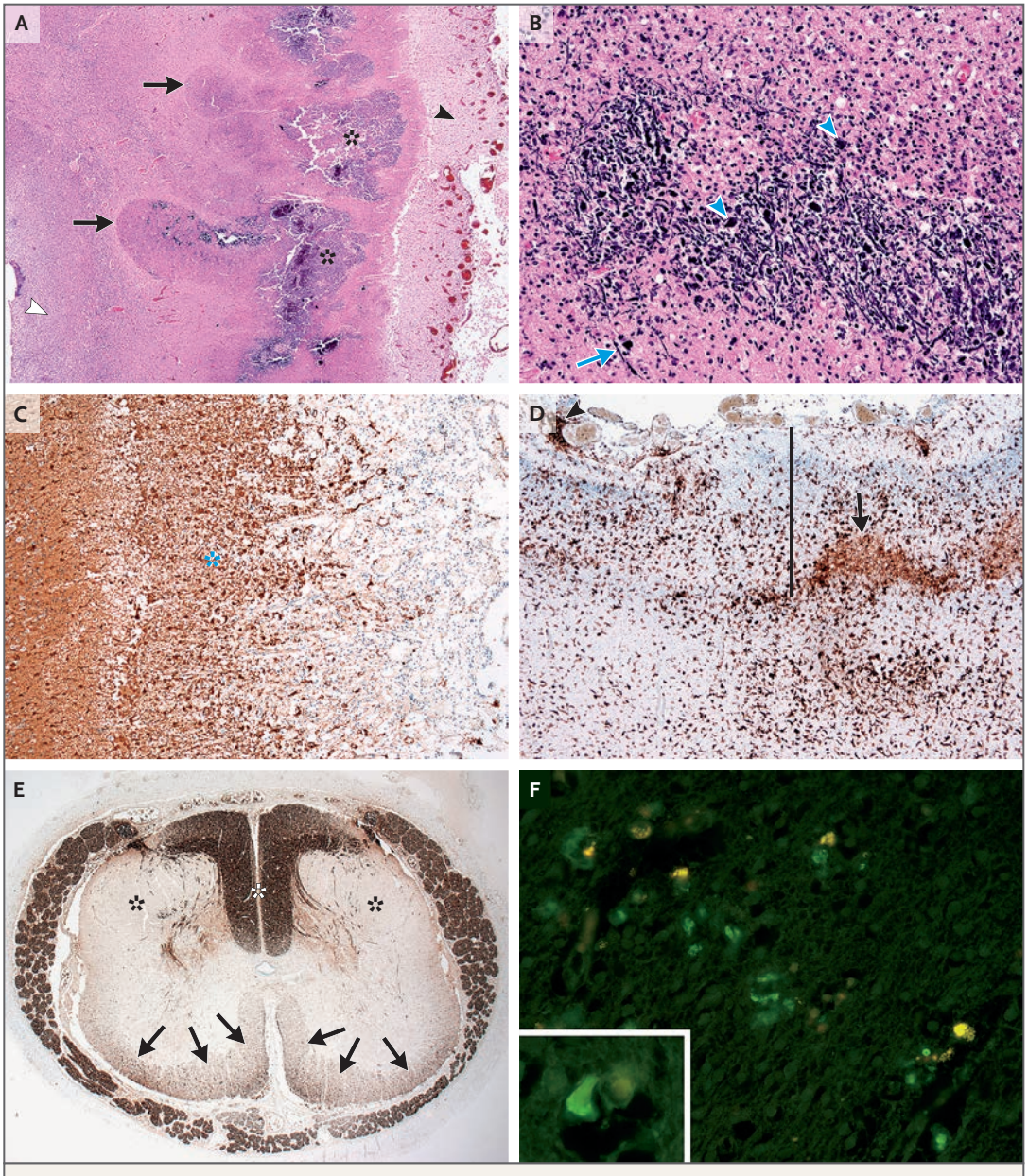

Figure 2. Microscopic Analysis of Brain Tissue.

Panel A shows thickened leptomeninges (black arrowhead) and irregular cortical and subcortical calcifications (asterisks) associated with cortical displacement (arrows), with preserved germinative matrix (white arrowhead); gyration is absent. Panel B shows higher magnification of calcifications with filamentous structures (arrow), possibly representing encrusted, damaged axons and dendrites, and oval and polygonal structures (arrowheads), possibly representing encrusted, damaged neuronal-cell bodies (hematoxylin and eosin staining in Panels A and B). Panel C shows immunohistochemical labeling of proliferated reactive astrocytes that extend into the subarachnoid space (asterisk) (glial fibrillary acid protein, clone 6F2 [Dako]). Panel D shows immunohistochemical labeling of numerous activated microglial cells and macrophages in the cortex (full thickness marked with a line) and subcortical white matter (lower part of the figure). Nonspecific staining of the calcifications is present (arrow). Focal leptomeningeal infiltrates of macrophages are seen (arrowhead) (HLA-DR, clone TAL 1B5 [Dako]). Panel E shows neurofilament immunohistochemical staining of axons in a cross-section of the lumbar spinal cord with severe Wallerian degeneration of the lateral corticospinal tracts (black asterisks), moderate involvement of other descending tracts (arrows), and well-preserved ascending tracts in the dorsal columns (white asterisk) (neurofilament, clone 2F11 [Dako]). Panel F shows indirect immunofluorescence of fetal brain tissue, revealing a green granular intracytoplasmic reaction (see also inset). The yellow signals adjacent to the green granules indicate autofluorescence of lipofuscin, suggesting that viral particles are located in the cytoplasm of neurons.

The New England Journal of Medicine
Downloaded from nejm.org on February 19, 2016. For personal use only. No other uses without permission.
Copyright © 2016 Massachusetts Medical Society. All rights reserved.

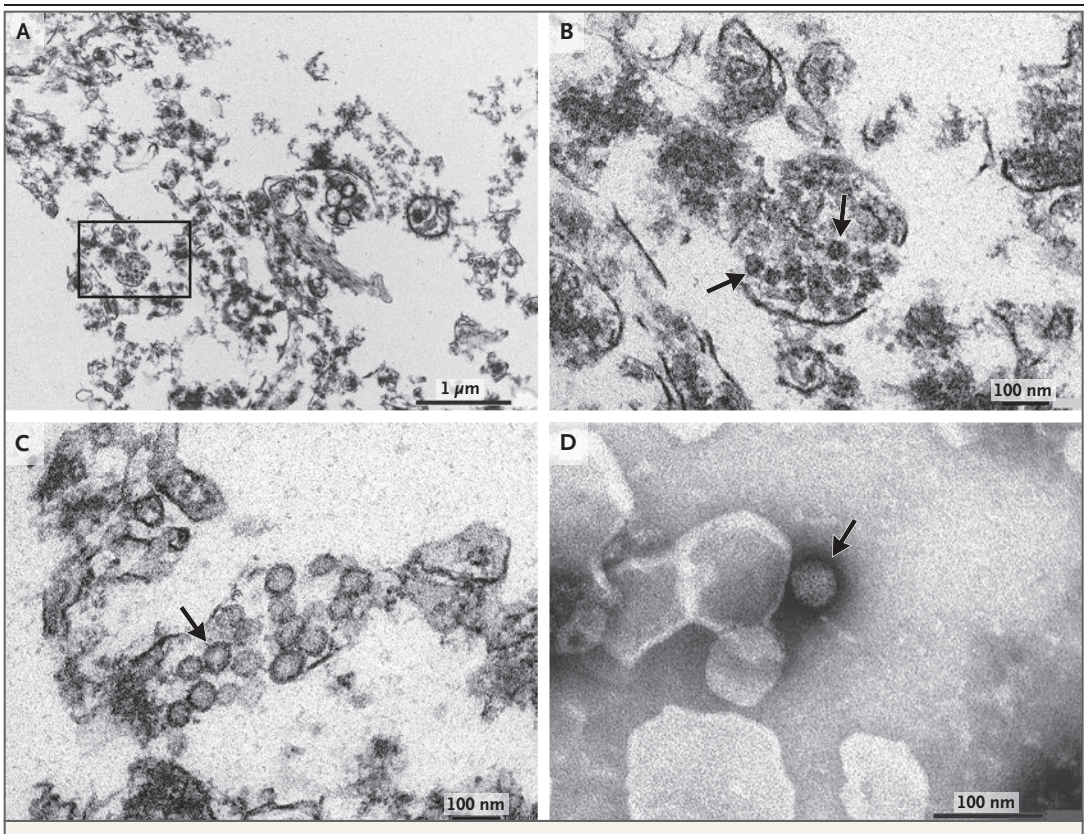

Figure 3. Electron Microscopy of Ultrathin Sections of Fetal Brain and Staining of a Flavivirus-like Particle.
Panel A shows a damaged brain cell with a cluster of dense virions located in the disrupted endoplasmic reticulum. Remains of membranes derived from different cellular compartments and filamentous structures are also seen. A magnified view of the boxed area with virions clearly visible (arrows) is shown in Panel B. Panel C shows a group of enveloped structures with a bright interior, presumably indicating viral replication (arrow). Panel D shows a negatively stained viral particle with morphologic characteristics consistent with those of Flaviviridae viruses (arrow).

and ZIKV detected in Sao Paolo, Brazil, in 2015 (KU321639), followed by a strain isolated in Cambodia in 2010 (JN860885, with 98.3% identity) and with a strain from the outbreak in Micronesia in 2007 (EU545988, with 98% identity) (Fig. 4). In the ZIKV polyprotein, 23 polymorphisms were detected in comparison with the strain from Micronesia and 5 polymorphisms in comparison with the isolate from French Polynesia; three amino acid changes were found in the NS1 region (K940E, T1027A, and M1143V), one in the NS4B region (T2509I), and one in the FtsJ-like methyltransferase region (M2634V).

DISCUSSION

This case shows severe fetal brain injury associated with ZIKV infection with vertical transmission. Recently, ZIKV was found in amniotic fluid of two fetuses that were found to have microcephaly, which was consistent with intrauterine transmission of the virus.[10] Described cases are similar to the case presented here and were characterized by severely affected CNS and gross intrauterine growth retardation. Calcifications in the placenta and a low placental–fetal weight ratio,[11] which were seen in this case, indicate potential damage to the placenta by the virus. Among the few reports of teratogenic effects of flaviviruses, investigators described the brain and eyes as the main targets.[12,13] No presence of virus and no pathological changes were detected in any other fetal organs apart from the brain, which suggests a strong neurotropism of the virus.

The localization of immunofluorescence signal and the morphologic appearance of the calcifications, which resembled destroyed neuronal structures, indicate a possible location of the

The New England Journal of Medicine
Downloaded from nejm.org on February 19, 2016. For personal use only. No other uses without permission.
Copyright © 2016 Massachusetts Medical Society. All rights reserved.

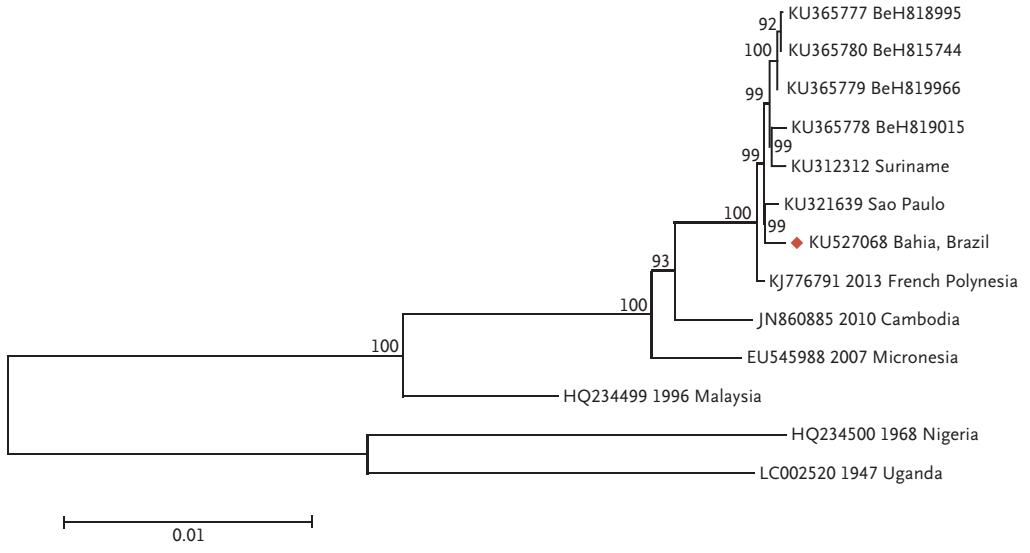

Figure 4. Phylogenetic Analysis of the Complete Genome of Zika Virus.

The evolutionary history was inferred by means of the neighbor-joining method under a GTR+G+I substitution model. The percentage of replicate trees in which the associated taxa clustered together in the bootstrap test (2000 replicates) is shown next to the branches. The GenBank accession number, year of isolation, and country of origin are indicated on the ZIKV branches for all strains except for those identified in 2015 and 2016. ZIKV strain Bahia, Brazil (KU527068), was obtained in this study. The complete genome sequence was recovered from fetal brain tissue. The 0.01 scale bar denotes the genetic distance in nucleotide substitutions per site.

virus in neurons. The consequent damage might cause arrested development of the cerebral cortex at the embryonic age of approximately 20 weeks.[14] The mechanism involved in the neurotropism of ZIKV is currently not clear. The association between ZIKV infection and fetal brain anomalies was also noted by findings on electron microscopy that were consistent with ZIKV detection in the fetal brain. Dense particles consistent with ZIKV were seen in damaged endoplasmic reticulum. Groups of enveloped structures with a bright interior resembling the remains of replication complexes that are characteristic of flaviviruses[15,16] indicate viral replication in the brain. The findings on electron microscopy suggest a possible persistence of ZIKV in the fetal brain, possibly because of the immunologically secure milieu for the virus. The number of viral copies that were detected in the fetal brain were substantially higher than those reported in the serum obtained from adult ZIKV-infected patients[17] but similar to those reported in semen samples.[18]

The complete genome sequence of ZIKV that was recovered in this study is consistent with the observation that the present strain in Brazil has emerged from the Asian lineage.[19] The presence of two major amino acid substitutions positioned in nonstructural proteins NS1 and NS4B probably represents an accidental event or indicates a process of eventual adaptation of the virus to a new environment. Further research is needed to better understand the potential implications of these observations. It is likely that the rapid spread of ZIKV around the globe will be a strong impetus for collaborative research on the biologic properties of the virus, particularly since the risk of neurotropic and teratogenic virus infections places a high emotional and economic burden on society.

Disclosure forms provided by the authors are available with the full text of this article at NEJM.org.

We thank the patient in this case for her willingness to provide detailed medical and immunologic data; Miha Juvan for processing of brain photographs; Peter Štrafela for his assistance with the neuropathological analyses; Martin Sagadin, Tina Uršič, Nataša Toplak, Simon Koren, and Andrej Steyer for their assistance in virus detection, sequencing, and analysis of next-generation sequencing data; Mateja Jelovšek for her assistance in comprehensive serologic investigations, and Luca Lovrečič and Marija Volk for their assistance in molecular karyotyping with microarray testing.

The New England Journal of Medicine
Downloaded from nejm.org on February 19, 2016. For personal use only. No other uses without permission.
Copyright © 2016 Massachusetts Medical Society. All rights reserved.

REFERENCES

1. Dick GW, Kitchen SF, Haddow AJ. Zika virus. I. Isolations and serological specificity. Trans R Soc Trop Med Hyg 1952;46:509-20.
2. Hayes EB. Zika virus outside Africa. Emerg Infect Dis 2009;15:1347-50.
3. Duffy MR, Chen TH, Hancock WT, et al. Zika virus outbreak on Yap Island, Federated States of Micronesia. N Engl J Med 2009;360:2536-43.
4. Cao-Lormeau VM, Roche C, Teissier A, et al. Zika virus, French Polynesia, South Pacific, 2013. Emerg Infect Dis 2014;20:1085-6.
5. Rapid risk assessment: Zika virus epidemic in the Americas: potential association with microcephaly and Guillain-Barré syndrome. Stockholm: European Centre for Disease Prevention and Control, December 10, 2015 (http://ecdc.europa.eu/en/publications/Publications/zika-virus-americas-association-with-microcephaly-rapid-risk-assessment.pdf).
6. Ioos S, Mallet HP, Leparc Goffart I, Gauthier V, Cardoso T, Herida M. Current Zika virus epidemiology and recent epidemics. Med Mal Infect 2014;44:302-7.
7. Faye O, Faye O, Diallo D, Diallo M, Weidmann M, Sall AA. Quantitative real-time PCR detection of Zika virus and evaluation with field-caught mosquitoes. Virol J 2013;10:311.
8. Faye O, Faye O, Dupressoir A, Weidmann M, Ndiaye M, Alpha Sall A. One-step RT-PCR for detection of Zika virus. J Clin Virol 2008;43:96-101.
9. Tamura K, Stecher G, Peterson D, Filipski A, Kumar S. MEGA6: Molecular Evolutionary Genetics Analysis version 6.0. Mol Biol Evol 2013;30:2725-29.
10. Oliveira Melo AS, Malinger G, Ximenes R, Szejnfeld PO, Alves Sampaio S, Bispo de Filippis AM. Zika virus intrauterine infection causes fetal brain abnormality and microcephaly: tip of the iceberg? Ultrasound Obstet Gynecol 2016;47:6-7.
11. Macdonald EM, Koval JJ, Natale R, Regnault T, Campbell MK. Population-based placental weight ratio distributions. Int J Pediatr 2014;2014:291846.
12. Alpert SG, Fergerson J, Noël LP. Intrauterine West Nile virus: ocular and systemic findings. Am J Ophthalmol 2003;136:733-5.
13. Tsai TF. Congenital arboviral infections: something new, something old. Pediatrics 2006;117:936-9.
14. Chi JG, Dooling EC, Gilles FH. Gyral development of the human brain. Ann Neurol 1977;1:86-93.
15. Goldsmith CS, Ksiazek TG, Rollin PE, et al. Cell culture and electron microscopy for identifying viruses in diseases of unknown cause. Emerg Infect Dis 2013;19:886-91.
16. Gillespie LK, Hoenen A, Morgan G, Mackenzie JM. The endoplasmic reticulum provides the membrane platform for biogenesis of the flavivirus replication complex. J Virol 2010;84:10438-47.
17. Lanciotti RS, Kosoy OL, Laven JJ, et al. Genetic and serologic properties of Zika virus associated with an epidemic, Yap State, Micronesia, 2007. Emerg Infect Dis 2008;14:1232-9.
18. Musso D, Roche C, Robin E, Nhan T, Teissier A, Cao-Lormeau VM. Potential sexual transmission of Zika virus. Emerg Infect Dis 2015;21:359-61.
19. Faye O, Freire CC, Iamarino A, et al. Molecular evolution of Zika virus during its emergence in the 20th century. PLoS Negl Trop Dis 2014;8(1):e2636.

Copyright © 2016 Massachusetts Medical Society.

The New England Journal of Medicine
Downloaded from nejm.org on February 19, 2016. For personal use only. No other uses without permission.
Copyright © 2016 Massachusetts Medical Society. All rights reserved.